9th International Interdisciplinary Congress on Renewable Energies, Industrial Maintenance, Mechatronics and Informatics

Booklets

RENIECYT
Registro Nacional de Instituciones y Empresas Científicas y Tecnológicas
1702902 CONAHCYT

RENIECYT - LATINDEX - Research Gate - DULCINEA - CLASE - Sudoc - HISPANA - SHERPA UNIVERSIA - Google Scholar DOI - REDIB - Mendeley - DIALNET - ROAD - ORCID - V|LEX

Title: Dynamic evaluation of composite roofs: Thermal optimization with PCM under extreme climate conditions

Authors: López-Salazar, Samanta, Simá, E., Chagolla-Aranda, M.A., Chávez-Chena, Y

TecNM/CENIDET LBH-6330-2024 0009-0004-9880-5145 918135
TecNM/CENIDET JZS-9886-2024 0000-0001-7601-1273 83891
TecNM/CENIDET LBI-3033-2024 0000-0002-7649-7389 368646
TecNM/CENIDET LBH-6345-2024 0000-0003-3348-397X 37563

Editorial label ECORFAN: 607-8695
BCIERMMI Control Number: 2024-01
BCIERMMI Classification (2024): 241024-0001
RNA: 03-2010-032610115700-14
Pages: 18

CONAHCYT classification:
Area: Engineering
Field: Engineering
Discipline: Mechanical Engineering
Subdiscipline: Thermal Engineering

ECORFAN-México, S.C.
Park Pedregal Business. 3580, Anillo Perif., San Jerónimo Aculco, Álvaro Obregón, 01900 Ciudad de México, CDMX,
Phone: +52 1 55 6159 2296
Skype: ecorfan-mexico.s.c.
E-mail: contacto@ecorfan.org
Facebook: ECORFAN-México S. C.
Twitter: @EcorfanC

www.ecorfan.org

Holdings
Mexico Colombia Guatemala
Bolivia Cameroon Democratic
Spain El Salvador Republic
Ecuador Taiwan of Congo
Peru Paraguay Nicaragua

Content

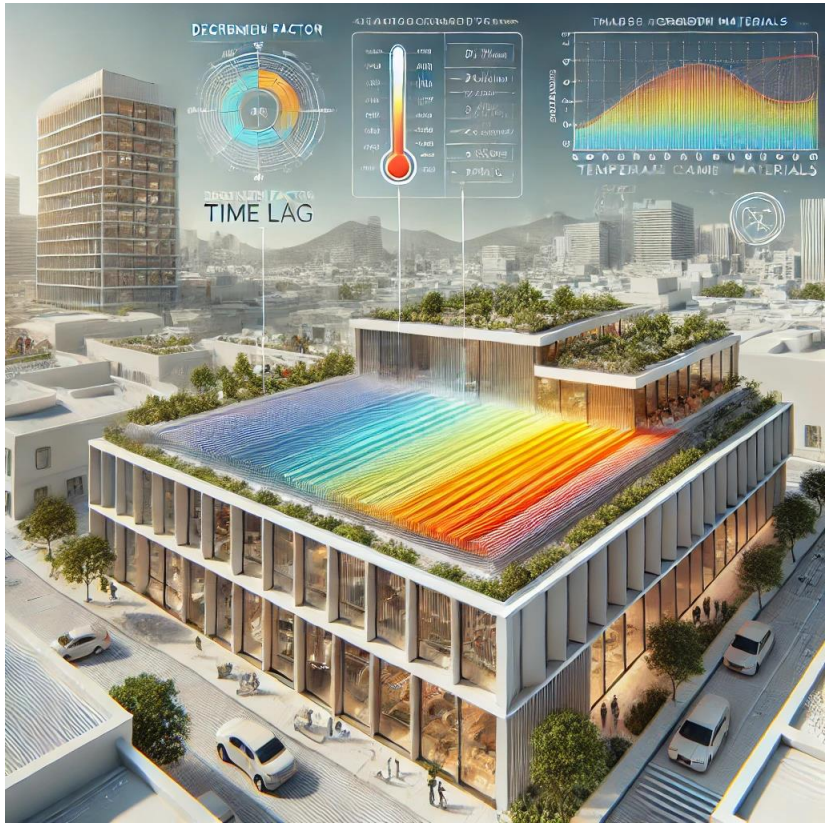

Introduction
Problem relevance

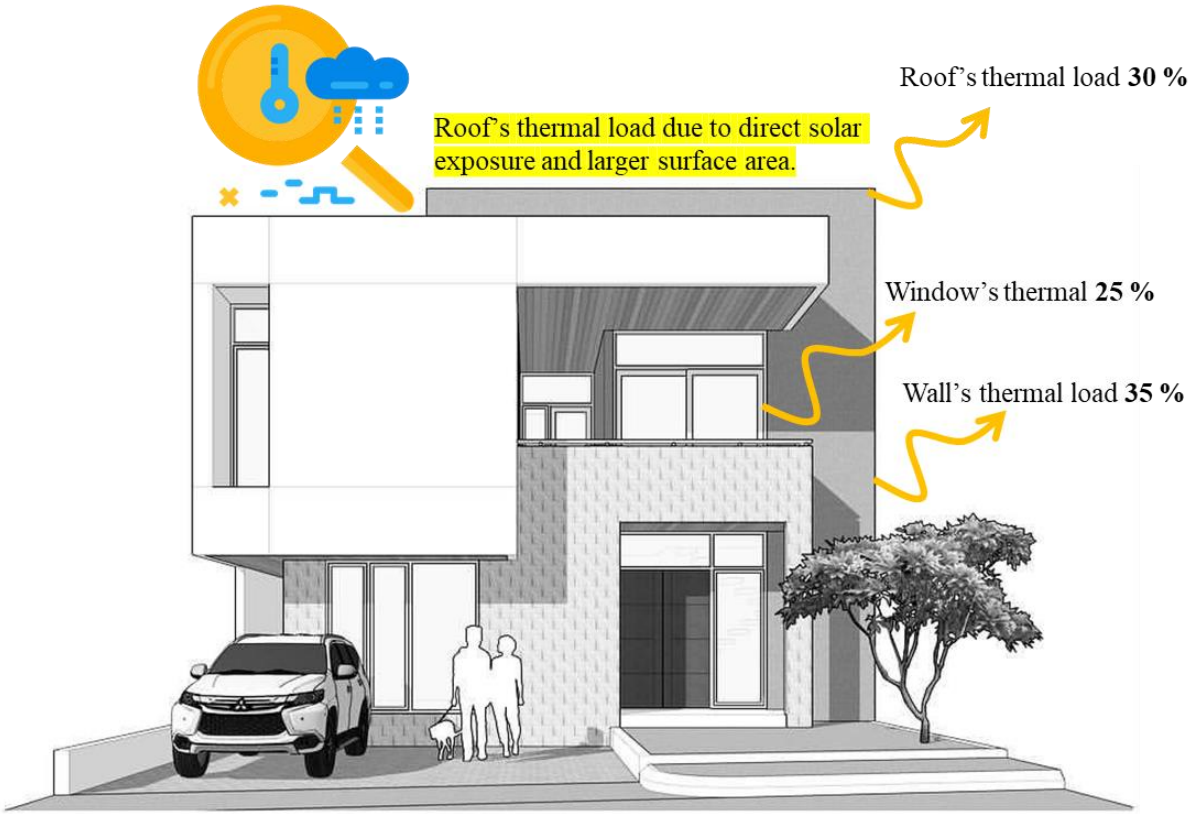

Figure. Distribution of thermal load contributions in a residential building (source: Shove et al., 2014).

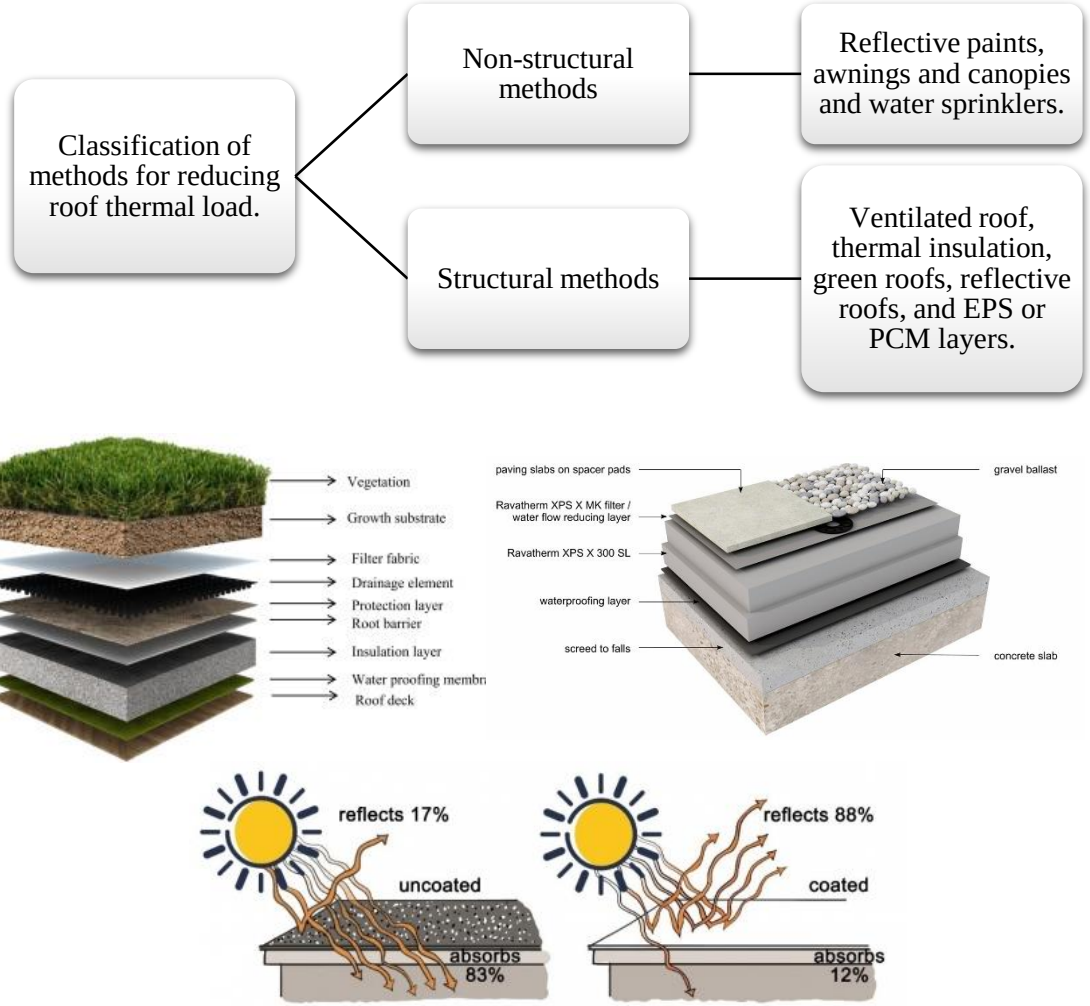

Figure. Classification of structural and non-structural methods for reducing roof thermal load (source: own elaboration).

Introduction
Phase Change Materials (PCM's)

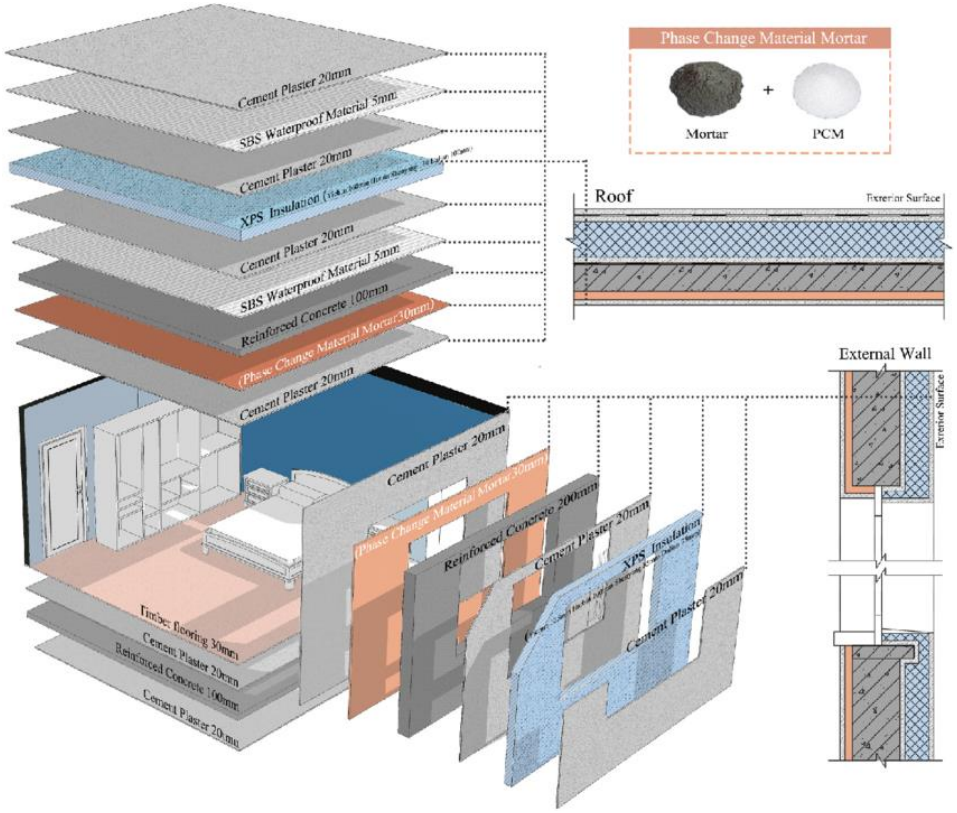

Figure. Structural composition of roof and external wall incorporating Phase Change Material Mortar and XPS insulation layers (source: Yu et al., 2023).

Phase Change Materials (PCMs) enhance thermal management in construction by absorbing, storing, and releasing latent heat during phase changes, effectively regulating indoor temperatures, especially in walls and roofs.

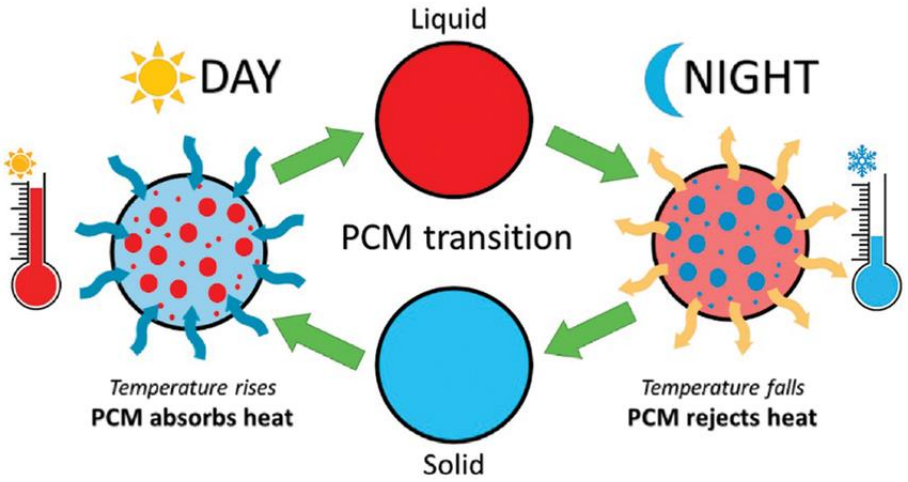

Figure. Phase transition of PCM in hot climates (source: Paul et al., 2022).

Introduction
Literature review

- **Piselli et al.:** la aplicación de PCM en membranas para techo reduce la temperatura superficial y el flujo de calor.
- **Bhamare et al.:** la inclinación de 2° de una capa PCM optimiza la carga térmica y mejor el ciclo de cambio de fase.
- **Qu et al.:** el grosor y la disposición óptimos del PCM en envolventes presenta ahorros de hasta 34.8 %.
- **Zahir et al.:** la selección y el encapsulamiento de PCM presenta desafíos en climas extremadamente cálidos.
- **Yu et al.:** el PCM reduce las horas de sobrecalentamiento y el consumo energético hasta en 19.7 % y 25.7 %, respectivamente.
- **Refahi et al.:** una doble capa de PCM con diferentes puntos de fusión ahorra un 6.6 % en calefacción y 2.8 % en refrigeración.

2019 → 2020 → 2021 → 2022 → 2023 → 2024

- **Arumugam & Shaik:** la combinación de PCM en techos y paredes reduce los costos de aire acondicionado y las emisiones.
- **Dardouri et al.:** en climas mediterráneos, se presentan ahorros de hasta 46.1 % con PCM, que depende del espesor y número óptimo de las capas.
- **Bhamare et al.:** el espesor óptimo de una capa de aire entre PCM es 2 cm.
- **Anter et al.:** PCM RT 35HC reduce la ganancia de energía hasta en 66 %.
- **Tang et al.:** combinar enfriamiento radiativo y PCM reduce la temperatura interior en 1.1 °C y la carga de enfriamiento en 172.9 %, eficiente para climas extremos.

Evaluated roof configurations

PCM selection

Table. Configuration overview: phases, material composition, and PCM thickness.

Phase 1
C1. (a) Ref
C2. (b) Ref+Ins
C3. (c) Ref+e10mmPCMi RT25 HC
C4. (c) Ref+e10mmPCMi RT35 HC*
C5. (c) Ref+e10mmPCMi RT44 HC
C6. (d) Ref+e10mmPCMo RT25 HC
C7. (d) Ref+e10mmPCMo RT35 HC*
C8. (d) Ref+e10mmPCMo RT44 HC
C9. (e) Ref+Ins+e10mmPCMi RT25 HC
C10. (e) Ref+Ins+e10mmPCMi RT35 HC*
C11. (e) Ref+Ins+e10mmPCMi RT44 HC
C12. (f) Ref+Ins+e10mmPCMo RT25 HC
C13. (f) Ref+Ins+e10mmPCMo RT35 HC*
C14. (f) Ref+Ins+e10mmPCMo RT44 HC
Phase 2, 20mm
C14-C16, e20 mmPCM
Phase 2, 30mm
C27 – C38, e30mmPCM
Phase 3
C39. (g) Ref+PCMi RT25 HC+PCMo RT25 HC
C40. (g) Ref+PCMi RT25 HC+PCMo RT35 HC*
C41. (g) Ref+PCMi RT25 HC+PCMo RT44 HC
C42. (h) Ref+PCMi RT25 HC+PCMo RT25 HC
C43. (h) Ref+PCMi RT35 HC*+PCMo RT25 HC
C44. (h) Ref+PCMi RT44 HC+PCMo RT25 HC
C45. (i) Ref+DoublePCMi bRT25 HC + tRT35 HC*
C46. (i) Ref+DoublePCMi bRT25 HC + tRT44 HC
C47. (j) Ref+DoublePCMi bRT35 HC* +tRT25 HC
C48. (j) Ref+Double PCMi bRT44 HC + tRT25 HC
C40. (i) Ref+DoublePCMo bRT25 HC + tRT35 HC*
C50. (i) Ref+DoublePCMo bRT25 HC + tRT44 HC

RT25 HC, RT35 HC*, and RT44 HC PCMs were selected to optimize thermal processes based on local temperatures.

- RT25 HC stabilizes indoor temperature at 25°C
- RT35 HC* mitigates daytime heat peaks around 35°C
- RT44 HC absorbs extreme outdoor heat near 44°C, enhancing energy efficiency and comfort.

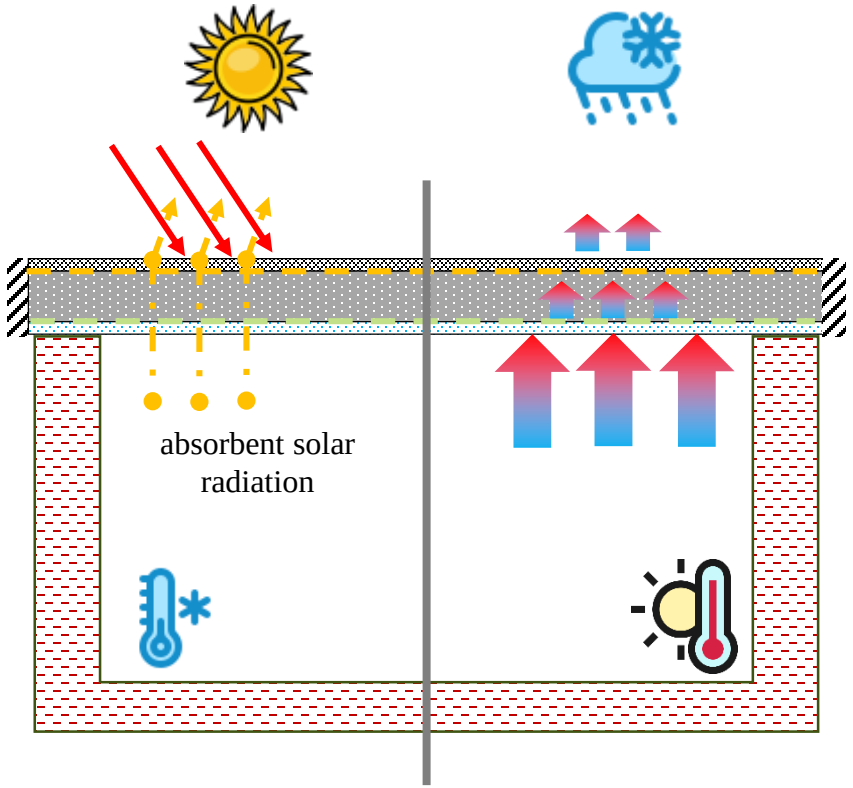

Evaluated roof configurations

Table. Thermophysical properties of each layer on the composite roof.

Material	λ, $Wm^{-1}°C^{-1}$	ρ, kgm^{-3}	C_P, $Jkg^{-1}°C^{-1}$	h_{ls}, Jkg^{-1}
Concrete	1.28	2200	850	-
Reinforced concrete	1.74	2300	920	-
Gypsum plaster	0.40	1200	837	-
Polystyrene insulation	0.03	28	1800	-
RT25 HC 22°C – 26 °C	0.20	880 770	2000	230 000
RT35 HC* 29°C – 36 °C		860 770		158 000
RT44 HC* 41°C – 44 °C		800 700		248 000

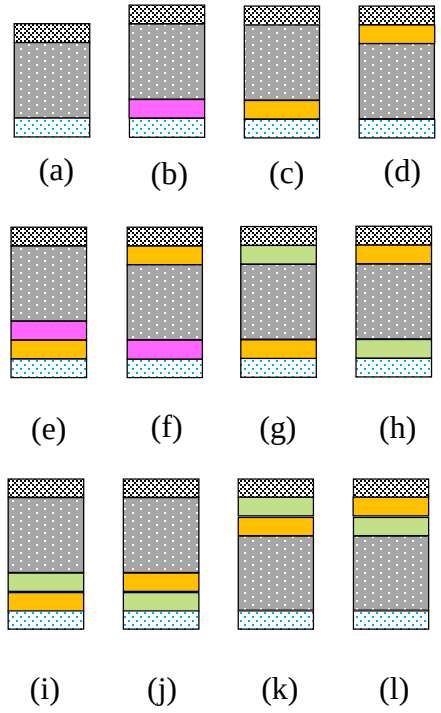

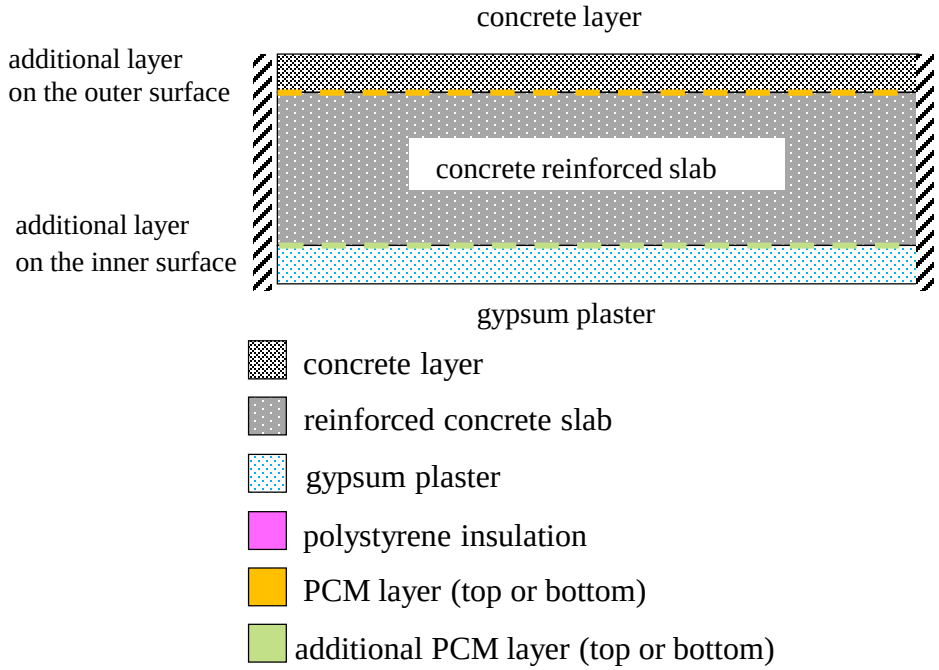

Figure. Cross section and configurations of a composite roof: reinforced concrete slab with concrete and gypsum plaster coats. And layer materials and locations (source: own elaboration).

Physical and mathematical model

The two-dimensional heat conduction process across all system layers (concrete, gypsum plaster, reinforced concrete, insulation, and PCM) is modeled by a mathematical equation, with necessary adjustments for the phase change in the PCM.

$$\frac{\partial(\rho C_P T)}{\partial t} = \frac{\partial}{\partial x}\left(\lambda \frac{\partial T}{\partial x}\right) + \frac{\partial}{\partial y}\left(\lambda \frac{\partial T}{\partial x}\right) \quad \text{Eq. (1)}$$

$$\frac{\partial(\rho_{PCM} C_{Peff} T_{PCM})}{\partial t} = \frac{\partial}{\partial x}\left(\lambda_{PCM} \frac{\partial T_{PCM}}{\partial x}\right) + \frac{\partial}{\partial y}\left(\lambda_{PCM} \frac{\partial T_{PCM}}{\partial x}\right) \quad \text{Eq. (2)}$$

$$C_{Peff} = \begin{cases} C_{Ps} & \text{for } T < (T_m - \Delta T) \\ \frac{C_{Ps} + C_{Pl}}{2} + \frac{h_{ls}}{2\Delta T} & \text{for } (T_m - \Delta T) < T < (T_m + \Delta T) \\ C_{Pl} & \text{for } T > (T_m + \Delta T) \end{cases} \quad \text{Eq. (3)}$$

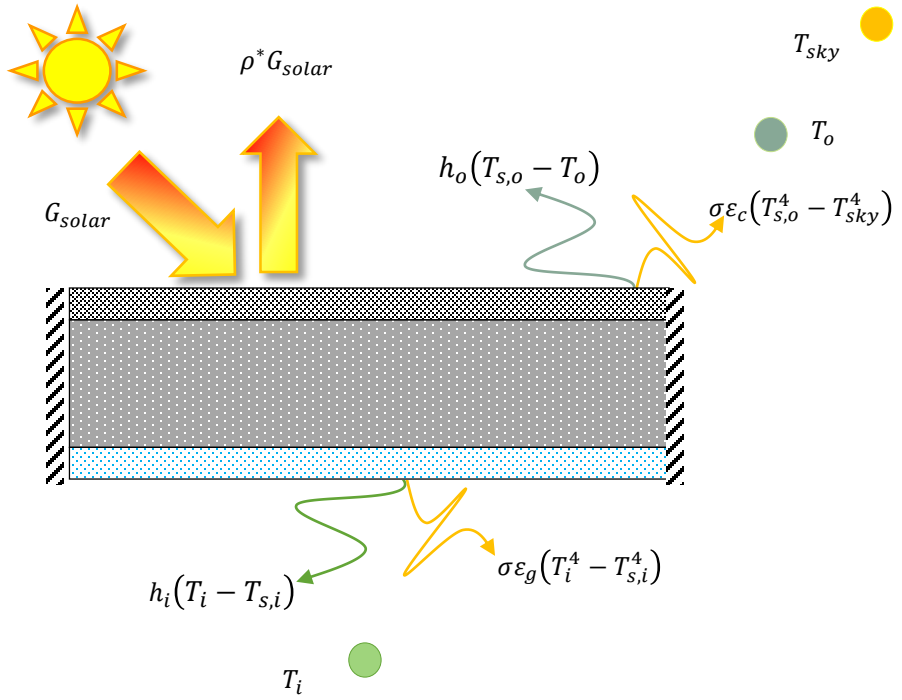

Figure. Heat transfer process on a composite roof subject to outside environmental conditions and at constant temperature on the inside surface (source: own elaboration).

Boundary conditions include solar radiation, wind-dependent convection, and heat transfer, with variations based on surface temperature.

$$-\frac{\partial T}{\partial y} = \alpha^* G_{solar} + h_o(T_{s,o} - T_o) + \varepsilon\sigma(T_{s,o}^4 - T_{sky}^4) \quad \text{Eq. (4)}$$

$$-\frac{\partial T}{\partial y} = h_i(T_i - T_{s,i}) + \varepsilon\sigma(T_i^4 - T_{s,i}^4) \quad \text{Eq. (5)}$$

Decrement Factor, Time Lag and Thermal Load

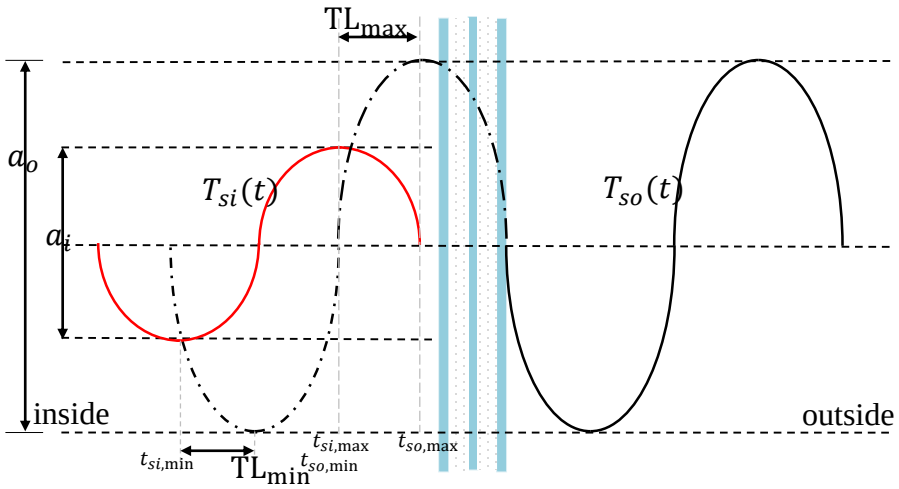

Figure. Schematic representation of the time lag, TL, and decrement factor, DF (source: own elaboration).

- Decrement factor: the radio of the temperature fluctuation amplitude on the interior surface to that on the exterior surface.
- Time lag: the delay between a temperature change on the exterior surface and the corresponding change on the interior surface.
- Thermal load: the amount of heat that needs to be added or removed to maintain the desired indoor temperature.

$$TL_{min} = t_{si,min} - t_{so,min} \quad (6)$$

$$TL_{max} = t_{si,max} - t_{so,max} \quad (7)$$

$$DF = \frac{a_i}{a_o} = \frac{T_{si,max} - T_{si,min}}{T_{so,max} - T_{so,min}} \quad (8)$$

Weather data

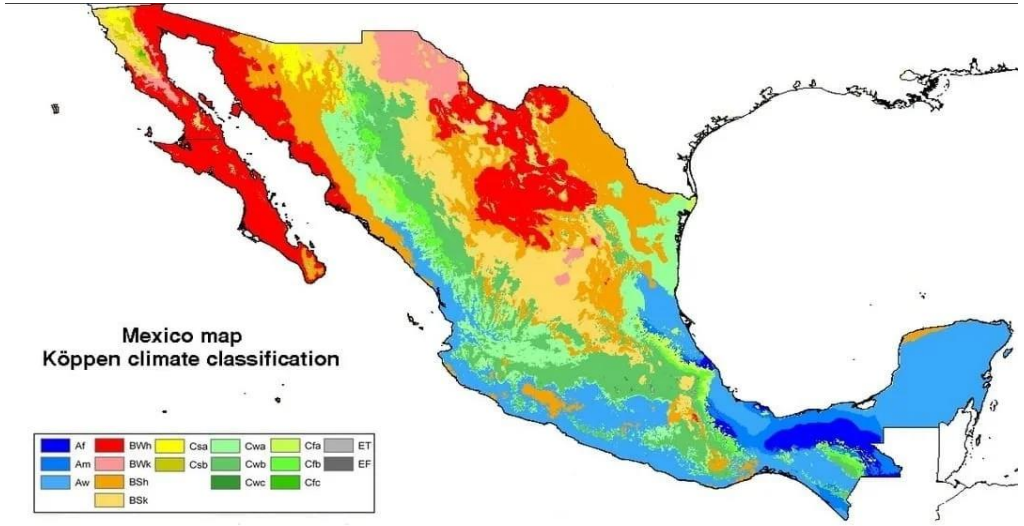

DISTRIBUCIÓN DE LA POBLACION SEGÚN EL CLIMA
POPULATION DISTRIBUTION ACCORDING TO CLIMATE

	Clima / Climate	Población / Population	% del total / % of total	
Templado todo el año de montaña	Cwb	28,662,545	35.4%	Temperate all year long highland
Cálido semiárido	BSh	11,803,982	14.6%	Hot semi-arid
Sabana	Aw	10,529,199	13.0%	Savanna
Subtropical subhúmedo	Cwa	10,110,335	12.5%	Subhumid subtropical
Estepa fría	BSk	6,459,358	8.0%	Cold Steppe
Desierto cálido	BWh	5,801,025	7.2%	Hot desert
Mediterráneo con verano cálido	Csa	2,074,662	2.6%	Hot-summer mediterranean
Monzónico	Am	1,989,843	2.5%	Monsoon
Desierto frío	BWk	1,391,180	1.7%	Cold desert
Oceánico	Cfb	1,115,743	1.4%	Oceanic
Subtropical húmedo	Cfa	868,014	1.1%	Humid subtropical
Selva	Af	227,677	0.3%	Rainforest
Tropical	A	12,746,719	15.7%	Tropical
Árido	B	25,455,545	31.4%	Arid
Rango Templado	C	42,831,299	52.9%	Temperate Range
Subtropical	Ca	13,053,011	16.1%	Subtropical
Templado todo el año	Cb	29,778,288	36.7%	Temperate all year long

Figure. Population distribution in Mexico according to Köppen climate classification (source: INEGI

The BWk cold desert climate of Ciudad Juarez, Mexico, was selected for this study due to its extreme temperature variations. The analysis focused on critical days with temperatures from -7.9°C to 46.1°C to evaluate roof thermal performance under these conditions, ensuring relevance to similar climates in Mexicali and Hermosillo.

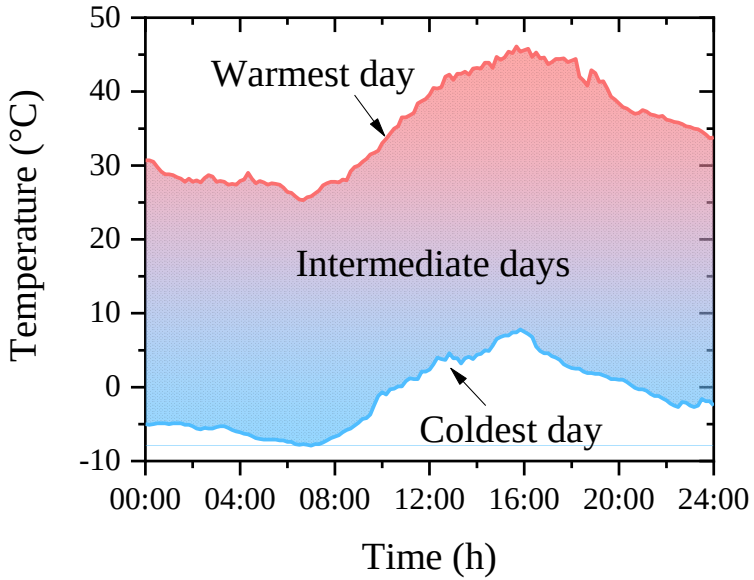

Figure. Recorded temperature interval: comparison respect to the climate spectrum of the region. Source: Own elaboration.

Methodology

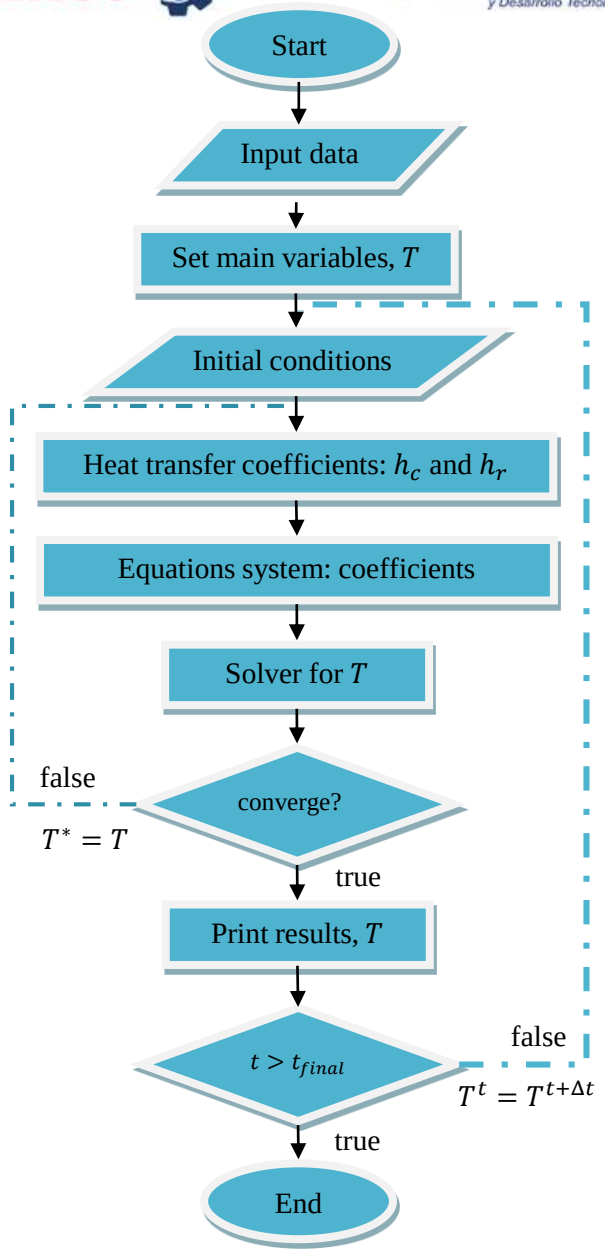

Figure. Numerical simulation workflow for solving 2D heat conduction using the finite volume method.(source: own elaboration).

Time discretization employed a fully implicit scheme, and the diffusive term was discretized using a centered scheme. The algebraic equations were solved using the Alternate Directions Gauss-Seidel method (LGS-ADI), with a residual tolerance set at 10^{-8} to ensure accuracy.

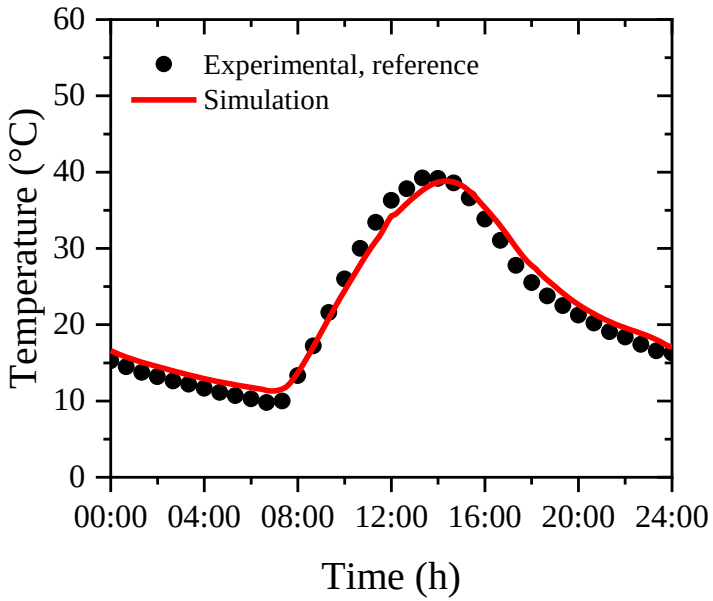

Figure. Surface temperature validation of a referenced roof compared to experimental data from Chagolla – Aranda et al., 2017 (source: own elaboration).

Results
Coldest day

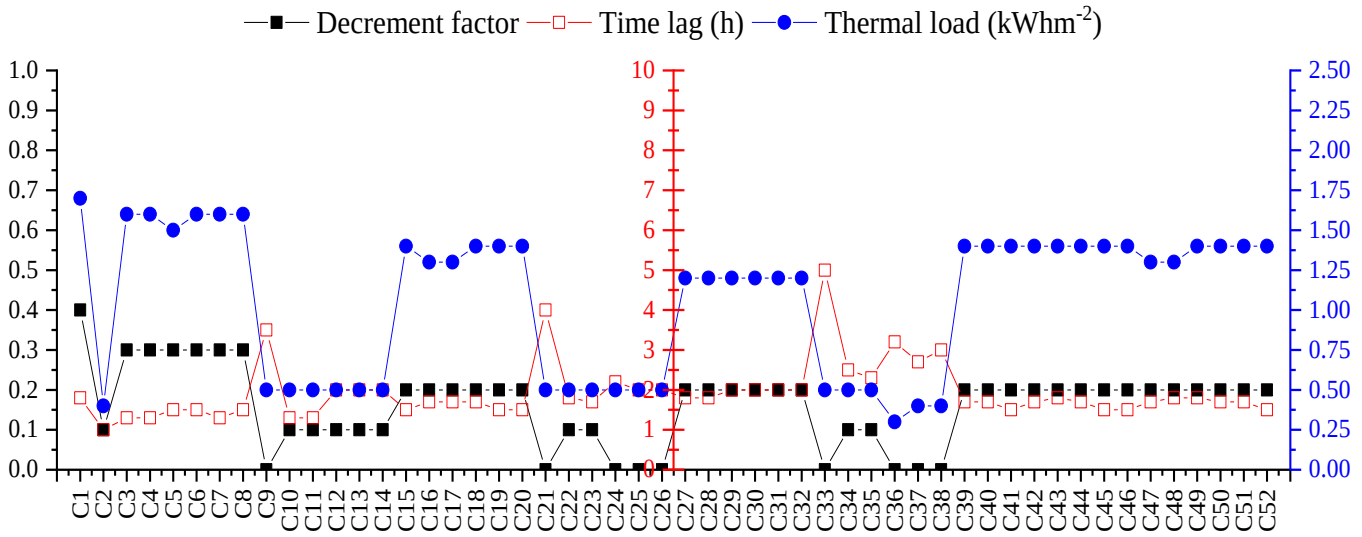

Figure. Comparison of the thermal performance on different roofs configurations under extreme weather conditions on the coldest day (source: own elaboration).

- Configurations with PCM on the inside surface (e.g., C3, C9) exhibit lower DF and longer TL, making them effective under cold conditions, though PCM does not reach melting, limiting phase change benefits.
- Increasing PCM thickness to 20 mm and 30 mm (e.g., C15, C38) further improves thermal attenuation and reduces heat loss.
- Double PCM layer configurations (e.g., C39, C45) demonstrate the best thermal performance, maintaining stable indoor temperatures in extreme cold.

Results
Warmest day

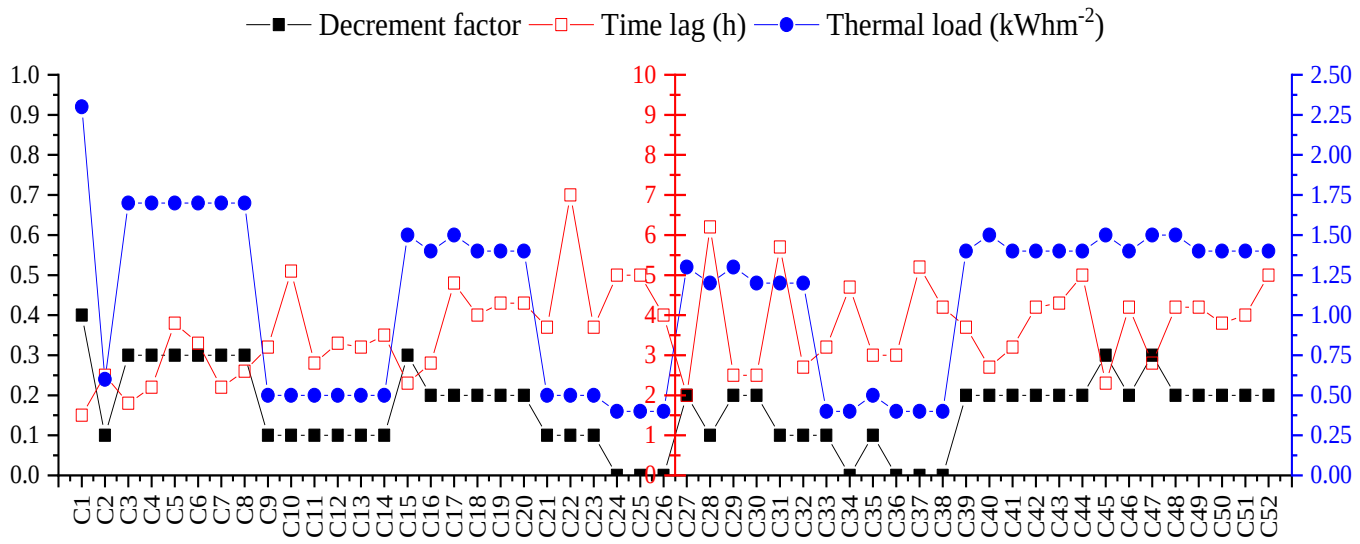

Figure. Comparison of the thermal performance on different roofs configurations under extreme weather conditions on the warmest day (source: own elaboration).

- On the warmest day, PCM effectively regulates heat gain through phase change, reducing thermal load.
- Configurations with PCM on the outside surface (e.g., C7, C13) limit heat gain effectively.
- Increasing PCM thickness (e.g., C28, C34) further enhances performance by reducing thermal load in high temperatures.
- Double PCM layer configurations (e.g., C40, C47) provide the best results, extending time lag and maintaining comfortable indoor temperatures under extreme temperature conditions.

Results
Comparision

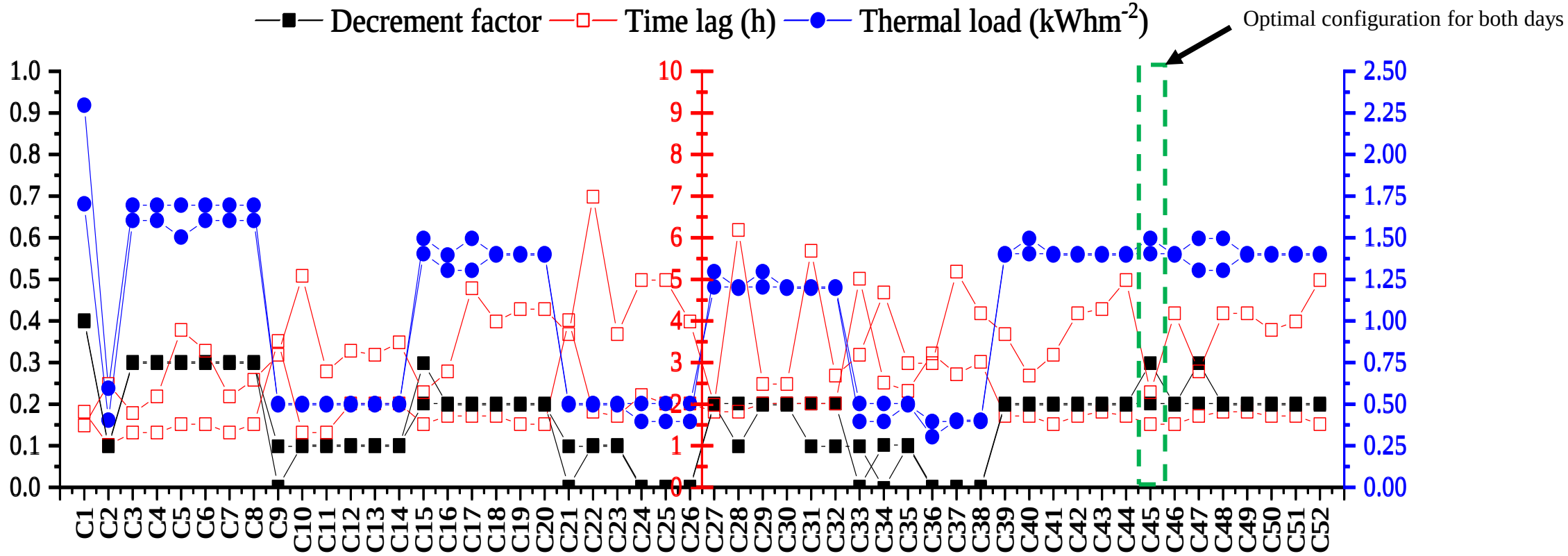

Results
Optimal configuration

Configuration C45, with a double PCM layer (RT25 HC inside, RT35 HC* outside), is the most efficient for extreme cold and warm conditions. It retains heat on cold days and limits heat gain on warm days, using phase change to manage thermal load effectively. This versatility makes C45 the best option for thermal comfort and energy efficiency.

1. **C39 (Double PCM Layer)**: Second-best option, balancing heat conservation and thermal gain reduction.
2. **C9 (Single PCM Layer with Insulation)**: Third-best, excels in heat conservation on cold days.
3. **C28 & C34 (Thicker PCM Layers)**: Good performance in reducing thermal loads on warm days.
4. **C3 & C7 (10 mm PCM)**: Acceptable but less effective in attenuating heat loss and limiting gain.
5. **C2 (Polystyrene Insulation)**: Moderate performance, less effective than PCM configurations.
6. **Best Overall**: C45 (Double PCM Layer) shows superior performance under extreme conditions.

Results
PCM vs Polystyrene comparison

On cold days, PCM outperforms polystyrene in insulation, time lag, and thermal load. On warm days, PCM better limits heat gain, making it superior for energy efficiency and comfort in fluctuating climates.

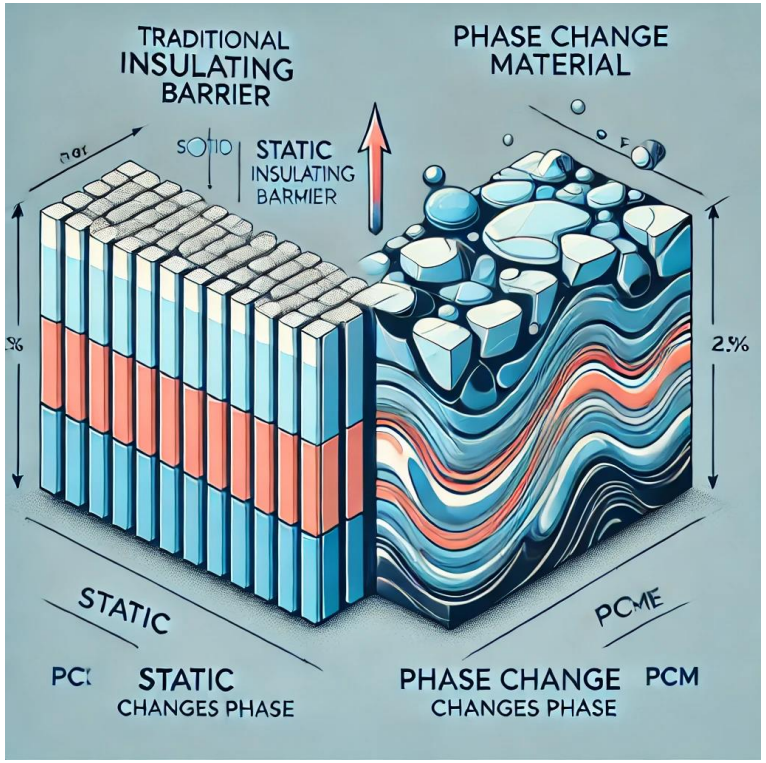

Results

Hierarchical order to improve the thermal efficiency of the roof begins with adding a PCM layer

Configurations with a PCM layer excel in thermal regulation, as they retain heat on cold days and limit heat gain on warm days. An increase in PCM thickness enhances thermal storage, extends time lag, and reduces thermal load. The addition of insulation further improves efficiency, while an extra PCM layer maximizes thermal performance, despite greater complexity and cost.

Conclusions

The results showed that PCM, especially with double layers or increased thickness, outperformed other methods.

- Optimal configurations achieved a decrement factor (DF) below 0.2, a time lag (TL) between 2 and 10 hours, and a thermal load under 2.5 kWh/m².
- Configuration C45, with dual PCM layers at 25°C and 35°C, proved most efficient under extreme conditions, surpassing polystyrene

Recommendations

Future studies could explore the use of PCM in combination with other advanced materials, as well as extending their application to other types of constructions and weather conditions, thereby widening the possibilities for thermal optimization and energy savings

ECORFAN®